Materials and Design 111 (2016) 640–645

Contents lists available at ScienceDirect

Materials and Design

journal homepage: www.elsevier.com/locate/matdes

Volumetric changes associated with B2-(Ni,Fe)Al dissolution in an Al-alloyed ferritic steel

Reza Rahimi [a], Péter Pekker [b], Horst Biermann [c], Olena Volkova [a], Bruno C. De Cooman [d], Javad Mola [a,*]

[a] Institute of Iron and Steel Technology, Technische Universität Bergakademie Freiberg, Germany
[b] Institute of Metal Forming Science and Nanotechnology, University of Miskolc, Hungary
[c] Institute of Materials Engineering, Technische Universität Bergakademie Freiberg, Germany
[d] Graduate Institute of Ferrous Technology, Pohang University of Science and Technology, Pohang, Gyeongbuk 790-784, South Korea

HIGHLIGHTS

- Anomalous length changes during continuous dilatometry heating of an Al-alloyed ferritic stainless steel were studied.
- The anomaly in the coefficient of thermal expansion was correlated with the precipitation and dissolution of B2-(Ni,Fe)Al intermetallics.
- Increase in the Al and Ni content of the ferritic matrix due to the dissolution of B2 intermetallics was responsible for the high apparent coefficients of thermal expansion.

GRAPHICAL ABSTRACT

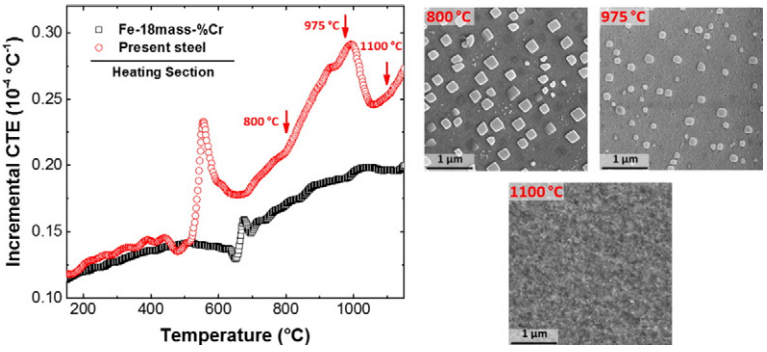

ARTICLE INFO

Article history:
Received 23 May 2016
Received in revised form 20 August 2016
Accepted 9 September 2016
Available online 10 September 2016

Keywords:
Al-alloyed steels
Stainless steels
Dilatometry
Coefficient of thermal expansion
B2-intermetallics

ABSTRACT

An Al-alloyed Fe–Cr–Ni–Al–Mn–C ferritic stainless steel exhibited a high apparent coefficient of thermal expansion during continuous heating in the temperature range of 800–1050 °C. The anomaly was ascribed to the matrix lattice expansion associated with the dissolution of (Ni,Fe)Al precipitates with a B2-CsCl crystal structure. The expansion was justified on the basis of the Al and Ni enrichment of the ferritic matrix as the precipitates dissolved.

1. Introduction

Steels containing up to about 10 mass-% Al have been designed for applications requiring a combination of high strength and ductility [1,2]. The density reduction caused by Al addition makes such steels attractive for a variety of applications particularly in the automobile industry where steel design concepts are driven by reduced fuel consumptions and exhaust emissions [3–6]. In cases where an austenitic rather than a duplex or a ferritic microstructure is desirable, the high ferrite potential of Al is compensated by the addition of a high carbon concentration [7]. The simultaneous presence of high concentrations of Al and C in high Mn steels in turn favors the formation of $(Fe,Mn)_3AlC_x$ kappa carbides in the austenite [8]. Kappa carbide is also

* Corresponding author.
E-mail address: mola@iest.tu-freiberg.de (J. Mola).

http://dx.doi.org/10.1016/j.matdes.2016.09.033
0264-1275/

the dominant type of carbide in ferritic steels containing Al, Mn, and C [2,9]. The ferrite phase of Al-alloyed high Mn duplex steels where the carbon partitions into the austenite, on the other hand, is prone to the formation of ordered intermetallic compounds most notably those of the type B2-FeAl and $D0_3$-Fe_3Al [10]. In particular, the formation of B2-intermetallic domains in ferrite, favored by the Ni addition [11], has been associated with promising mechanical properties.

In Al-alloyed ferritic steels containing high Ni contents, Fe in the B2-FeAl is partially replaced by Ni [11]. The formation of B2-(Ni,Fe)Al intermetallic precipitates in Fe–10Cr–10Ni–3.4Mo–(3 − 10)Al-base ferritic steels (values in mass-%) and its influence on the mechanical properties have been explored in many recent investigations [12–18]. In contrast to B2-intermetallics in high Mn steels which appears as domains in the ferrite hardly identifiable without diffraction analysis in transmission electron microscope (TEM) [8], B2-phase in the latter alloy system and in high Cr steels alloyed with Ni and Al [19–22] appears as discrete precipitates in the ferritic matrix. This enables their identification even by scanning electron microscopy. In certain commercial steels, for instance the stainless steel grade PH13-8 Mo, B2-intermetallics serve as strengthening second phase particles [23].

The dissolution and precipitation of B2-intermetallics have profound consequences for the mechanical properties of Al-alloyed steels [17,24]. Therefore, devising straightforward methods of studying the preceding reactions will eliminate the need for time-consuming microstructural examinations otherwise necessary for this purpose. Non-isothermal dilatometry is a powerful and yet quick method of analyzing solid-state phase transformation kinetics which relies on the identification of inflection points in dilatation data obtained at various heating rates [25]. This method has been used for instance for the analysis of tempering reactions in martensitic steels [25–27], dissolution of cementite in austenitic steels [28], and most commonly for the identification of critical temperatures such as A_1, A_3, and A_{cm} at different heating and cooling rates [29,30]. The present paper demonstrates a dilatometry-based method of studying the dissolution and precipitation of B2-intermetallics in an Al-alloyed stainless steel.

2. Methods

Al-added steel with the chemical composition shown in Table 1 was cast in a vacuum induction melting furnace. The cast ingot was homogenization annealed at 1200 °C for 1 h. Subsequent blow of N_2 gas yielded an average cooling rate of 2.5 °C/s in the temperature range 1200–600 °C. The microstructure was subsequently examined using a Neophot 30 type light optical microscope, a Zeiss Ultra 55 type field emission scanning electron microscope (FE-SEM), and an FEI Tecnai G2 type transmission electron microscope (TEM) operated at an acceleration voltage of 200 kV. Samples for TEM examinations were mechanically polished to a thickness of <100 μm and then twin-jet polished at room temperature (RT). X-ray diffraction (XRD) measurements with Cu K_α radiation were performed in a Seifert-FPM URD-6 diffractometer. Dilatometry studies using $3.5 \times 3.5 \times 10\ mm^3$ samples were done in a BÄHR-DIL805 dilatometer. Heating and soaking steps were done in vacuum before cooling with argon. Heating and cooling rates in dilatometry cycles were 50 °C/s and 20 °C/s, respectively. In-situ high temperature XRD measurements with Cu K_α radiation were conducted in a Bruker D8 diffractometer equipped with an Anton Paar heating stage. To minimize the oxidation, the specimen chamber was evacuated and backfilled with Ar.

Table 1
Chemical composition of the Al-added steel.

Element	C	Al	Mn	Cr	Ni	Si	Fe + others
mass-%	0.46	7.1	6.2	17.1	8.7	0.4	Balance
at.%	1.93	13.3	5.7	16.6	7.5	0.7	Balance

3. Results and discussions

The microstructure after homogenization treatment is shown in Fig. 1. The coarse precipitates readily visible in the optical micrograph of Fig. 1(a) have been shown elsewhere to be of the type M_7C_3, where M denotes Cr, Fe, and substitutional alloying elements [31]. The SEM micrograph in Fig. 1(b) reveals the presence of fine precipitates in the matrix of Fig. 1(a). Supplemental TEM examinations presented in Fig. 1(c) confirmed a bimodal distribution of coarse (~200 nm) and fine (<20 nm) precipitates in the matrix. Selected area electron diffraction (SAED) patterns of a coarse precipitate and a region of the matrix containing only a small fraction of fine precipitates are shown in Fig. 1(d) and 1(e), respectively. Both SAED patterns include reflections pertaining to the ordered B2-intermetallic phase with a cubic CsCl-type crystal structure. However, due to the presence of a lower volume fraction of B2-intermetallics, the intensity of their characteristic superlattice reflections is weaker in Fig. 1(e). The orientation relationship between the B2-intermetallics and the ferritic matrix is of the type cube-on-cube, namely $(011)_{B2}$ // $(011)_\alpha$ and $[0\bar{1}1]_{B2}$ // $[0\bar{1}1]_\alpha$. Quantitative energy dispersive spectroscopy analysis (EDS) in TEM revealed that the B2-intermetallics were enriched with Al and Ni (see Table 2).

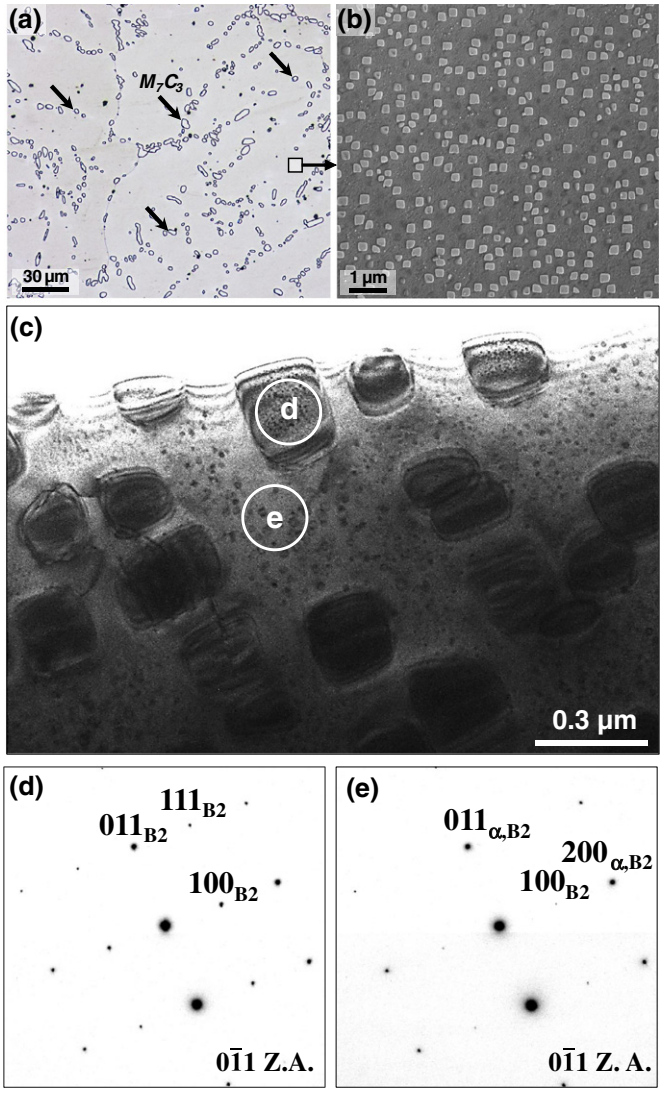

Fig. 1. (a) Optical micrograph showing an overview of the homogenized microstructure. (b) SEM and (c) TEM micrographs of the matrix in (a). (d–e) SAED patterns taken from the regions marked in (c).